International Journal of Signal Processing, Image Processing and Pattern Recognition
Vol. 10, No. 6 (2017), pp. 23-38
http//dx.doi.org/10.14257/ijsip.2017.10.6.03

# Monitoring Method of High-speed Tool Wear Level based on Machine Vision

Zeqing Yang[1], Libing Liu[1], Kai Peng[1*],Shanshan Li[1], Junfeng Zhang[1]and Liya Gai[2]

[1]*School of Mechanical Engineering, Hebei University of Technology, Tianjin 300130, P.R. China*
*yzq82@163.com,liulibing@hebut.edu.cn, kaip_tju@163.com, 954434271@qq.com, 18902098921@163.com*
[2]*Shenyang No.1 Machine Tool Works of Shenyang Machine Tool Group CO., LTD., Shenyang, 110142, China*
*liya_gai@smtcl.com*

***Abstract***

*In order to improve accuracy and efficiency of high-speed cutting tool wear monitoring and classification, the novel method was proposed to identify the tool wear level and estimate wear capacity based on machine vision and fuzzy statistical learning. Wear feature parameters were extracted by analyzing the high-speed cutting tool wear morphology and wear mechanism. The feature vector of each worn tool was established, and the membership functions were designed, which correspond with low, medium and high wear level. The method represents the probability of belonging to the low, medium and high wear level. Finally, we had experimented in high speed machining shaft on the HTC2550hs high-speed Computer Numerical Control (CNC) turning center in Shenyang Machine Tool Co.,LTD.. Experimental results show that the method can effectively identify the tool wear level, and identification accuracy can get 98.7%. The estimate of wear capacity provides an important basis for tool radius compensation when the wear level is located in the L class (low) level, and allows to replace the tool when the wear level is located at the end of the M class (medium), preventing that the tool enters into the H class (high).*

***Keywords****: High speed cutting-tool, cutting-tool wear, machine vision, monitoring, fuzzy pattern recognition*

## 1. Introduction

Tool condition monitoring is the key technology to ensure the product quality and the reliable operation of machining system in the process of high-speed CNC machining [1-2]. High-speed cutting tool must be withstood high pressure, high temperature, friction, impact and vibration *etc*., so the cutting tool wear morphology, wear mechanism and monitoring technology are very different from the constant speed cutting [3]. The tool wear degree was usually estimated by the workers according to the vibration or noise of the machine tool and cutting state. Most studies rely on experience; the scopes are also limited to the certain processing conditions. There are some general problems such as the inconvenience of installing, different process system with poor interchangeability, high cost *etc*. In high-speed processing, the high-speed rotating tools accumulate a large amount of energy and under the great centrifugal force, which will make the tool worn or broken sharply. In order to prevent the loss of workpiece surface quality caused by the

*Corresponding Author

ISSN: 2005-4254 IJSIP

excessive cutting-tool wear, avoid the faults such as workpiece scrapped or machine damage caused by tool breakage, the active monitoring technology must be taken in the work cycle for high-speed cutting tools and the wear level must be online recognize and control to ensure completion high-speed machining tasks with high quality, high efficiency and low consumption [4-6].

With the development of image processing technology, the high-speed cutting tool condition monitoring based on machine vision is gradually entering the field of mechanical automation. Machine vision is non-contact inspection method with integrated use of image processing, precision measurement, pattern recognition and artificial intelligence technology *etc* [7-8].It has many advantages, such as image processing capabilities with high-precision, the ability of identifying the different wear morphologies, the flexible of applying to different processing types, easy positioning on the machine, obtaining the precise amount of abrasion *etc*.. The directional light was frequently used for flank wear measurements with machine vision, the artificial neural networks were designed for automatic tool wear recognition using images of cutting tool [9]. Reference [10] presented a method for micro-milling tool wear inspection using machine vision, the geometrical measurements required to locate the cutting edges of the micro-tool and the variable light intensity was used during image acquisition to detect regions of different reflective properties. Geometrical information and reflective properties were then used to evaluate the tool wear.

In view of the problems of poor environment adaptation ability and single monitoring object, the new method was proposed to estimate wear capacity and tool wear level based on machine vision and fuzzy statistical learning, in order to improve accuracy and efficiency of high-speed cutting tool wear monitoring and classification, and meet the monitoring requirements of tool wear state in a variety of conditions, which providing an important basis for tool radius compensation and timely replacement the tool in machining.

## 2. High Speed Machining Tool Wear Morphologies and Feature Analysis

### 2.1. High Speed Machining Tool Wear Morphologies

The form of tool damage mainly is tool wear and tool breakage in high-speed cutting. The damage reason with the cutting tool material and workpiece material is different, mainly caused by abrasive wear, adhesive wear, chemical wear (oxidation, diffusion and dissolution, *etc*.), brittle breakage and plastic deformation under the cutting forces and heat [3,11]. The dominant wear morphology and wear mechanism are different under different cutting conditions with different workpiece materials. Research shown that the damage of the tool commonly is flank wear, front face crater wear, boundary wear and micro-chipping, tipping, flaking, cataclasm and the plastic deformation [3,12], as shown in Figure1. The main high-speed cutting tool materials are diamond, Cubic Boron Nitride (CBN) ceramics, TiC(N) cemented carbide (metal ceramics) and cemented carbide coating *etc*. [12]. When high-speed cutting the steel material, the most damage is the flank surface of cutting tool ground into facet and the rake face ground into the crater accompanied by micro-chipping[13,14]. When high-speed cutting the high-temperature alloy, hardened steel and very soft steel materials, the most damage is boundary wear [15]. It occurs in the cutting depths that is the contact edge of tool and workpiece, the shape is elongated groove known as the groove wear. When high-speed cutting the brittleness tools material, the most damage is the tool breakage.

### 2.2. Wear Feature Analysis

 

Taking the two typical wear forms as examples, the rake face was ground into the crater and the flank was ground into facet. The extraction of wear features were shown in Figure 2 and Figure 3. In Figure 2, KB is the width of crater wear, KM is the distance between the center of crater and the cutting edge, KT is the depth of the crater. In Figure 3, the flank wear was divided into three areas: tool point wear zone (C zone), middle wear zone (B zone) and boundary wear zone (N zone). In C zone, VC is the size of deputy wear trench caused by low intensity and temperature concentration near the tip. In B zone, VB is the average width of tool flank wear, VBmax is the maximum wear capacity of tool flank caused by friction and poor heat dissipation [16]. In N zone, the wear capacity VN at the juncture of cutting edges and the surface to be processed was wear groove size, which was caused by high-temperature oxidation and surface-hardened layer. So the seven parameter values KB, KM, KT, VB, VBmax, VN, VC were chosen as wear eigenvalue.

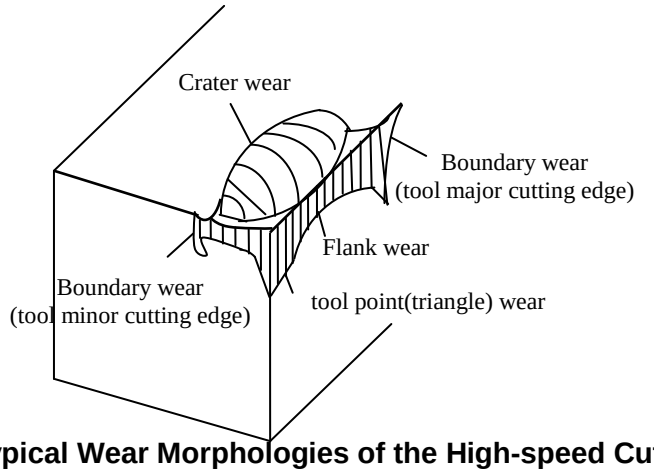


**Figure 1. Typical Wear Morphologies of the High-speed Cutting Tool**

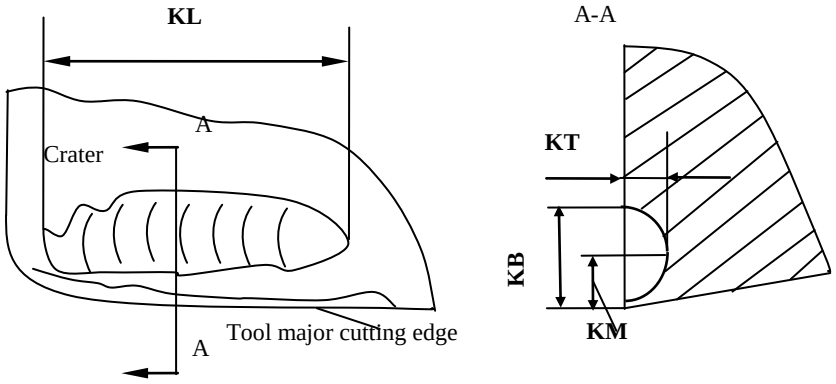


**Figure 2. Crater Wear Features of the Tool Rake Face**

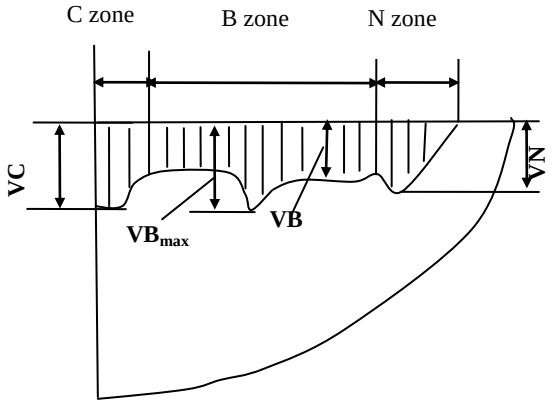


**Figure 3. The Tool Flank Wear Features**

### 2.3. Feature Description of Tool Wear Mode

The above seven parameters were used as wear eigenvalue; every tool wear shape eigenvector was expressed as Equation.1.

$$U = \{u_1, u_2, u_3, u_4, u_5, u_6, u_7\} \tag{1}$$

The wear mode was divided into three categories according to the degree of wear: low wear level (L), medium wear level (M) and high wear level (H) [17].

Extracting the number of samples m, n, k as learning samples from L, M, H was respectively expressed as Equation.2,3,4.

$$L = (l_{ij}) = \begin{bmatrix} l_{11} & l_{12} & \cdots & l_{17} \\ l_{21} & l_{22} & \cdots & l_{27} \\ \vdots & \vdots & \vdots & \vdots \\ l_{m1} & l_{m2} & \cdots & l_{m7} \end{bmatrix} \tag{2}$$

$$M = (m_{ij}) = \begin{bmatrix} m_{11} & m_{12} & \cdots & m_{17} \\ m_{21} & m_{22} & \cdots & m_{27} \\ \vdots & \vdots & \vdots & \vdots \\ m_{n1} & m_{n2} & \cdots & m_{n7} \end{bmatrix} \tag{3}$$

$$H = (h_{ij}) = \begin{bmatrix} h_{11} & h_{12} & \cdots & h_{17} \\ h_{21} & h_{22} & \cdots & h_{27} \\ \vdots & \vdots & \vdots & \vdots \\ h_{k1} & h_{k2} & \cdots & h_{k7} \end{bmatrix} \tag{4}$$

Calculating their average of each column was respectively expressed as Equation.5,6,7.

$$l = \{l_1, l_2, l_3, l_4, l_5, l_6, l_7\} \tag{5}$$

$$m = \{m_1, m_2, m_3, m_4, m_5, m_6, m_7\} \tag{6}$$

$$h = \{h_1, h_2, h_3, h_4, h_5, h_6, h_7\} \tag{7}$$

Where $l_j = \frac{1}{m}\sum_{i=1}^{m} l_{ij}\ (j = 1,2,\cdots 7)$, $m_j = \frac{1}{n}\sum_{i=1}^{n} n_{ij}\ (j = 1,2,\cdots 7)$, $h_j = \frac{1}{k}\sum_{i=1}^{k} h_{ij}\ (j = 1,2,\cdots 7)$.

$d(u,l), d(u,m), d(u,h)$ was respectively expressed as Equation.8,9,10,which were the distance between specific sample $U = \{u_1, u_2, u_3, u_4, u_5, u_6, u_7\}$ and l, m, h.

$$d(u,l) = \sqrt{\sum_{j=1}^{7} (u_j - l_j)^2} \tag{8}$$

 

$$d(u,m)=\sqrt{\sum_{j=1}^{7}(u_j-m_j)^2} \tag{9}$$

$$d(u,h)=\sqrt{\sum_{j=1}^{7}(u_j-h_j)^2} \tag{10}$$

L, M, H fuzzy sets' membership function is $\mu L(u), \mu M(u), \mu H(u)$ respectively in U, and their values are the values between 0 and 1. The membership function of L, M, H are selected as Equation.11,12,13 respectively.

$$\mu L(u)=1-\frac{d(u,l)}{d(u,l)+d(u,m)+d(u,h)} \tag{11}$$

$$\mu M(u)=1-\frac{d(u,m)}{d(u,l)+d(u,m)+d(u,h)} \tag{12}$$

$$\mu H(u)=1-\frac{d(u,h)}{d(u,l)+d(u,m)+d(u,h)} \tag{13}$$

### 2.4. The Monitoring Method of Tool Wear Level

The membership functions of different wear level were established based on fuzzy statistical method to describe tool image and analyze the learning samples. The testing sample's membership was calculated for monitoring tool wear levels in order to adopt the positive and effective measures. When the primary wear level (L level), the wear was calculated using the Equation.14.

$$V_B=\frac{\sum(P_i(x)-P_0(x))}{B}\times\alpha \tag{14}$$

Where $P_i(x)$ is the present boundary value which got form the picture of cutting tool, $P_o(x)$ is the initial boundary value, B is the width of B zone, $\alpha$ is the physical dimension corresponding to single pixel [18,19]. The amount of different material tool front and rear flank wear were obtained in the similar method according to the cutting condition and high speed cutting tool wear mechanism, which provide an important basis for tool radius compensation through modifying the corresponding bias parameters [20]. The tool should be replaced when the wear level is located at the end of the M level (medium), preventing that the tool enters into the H level (high).

## 3. Experimental Analysis

### 3.1. Tool Wear Monitoring Scheme based on Machine Vision

To verify the rationality and effectiveness of the algorithm, we had tested tool wear in high speed machining shaft on the high-speed Computer Numerical Control (CNC) turning center HTC2550hs in Shenyang Machine Tool Co.,LTD.. The Image obtaining program is shown in Figure 4. Tool wear monitoring system based on machine vision mainly consists of CCD camera, LED ring light source and microscope. The energy conservation and environmental protection high brightness LED ring light source was chosen in order to ensure the accuracy of identification and get clear front face and flank tool image. And the emitting light element was used as red LED with the higher color saturation and preferably monochromatic, which the dominant wavelength was about 625 nm, approximately the wavelength of CCD photosensitive element peak wavelength, and met the requirements of monochrome CCD with active lighting light source in lighting effect. The shell was designed for a ring structure, the inner diameter keep consistent with the outer diameter of the CCD camera, and can be set in the CCD and fixed together by hex screws, guaranteeing the relatively fixed position of the light source and the camera [21]. The XTL-1 stereo microscope was used with the diameter of the objective lens is

2cm and the magnification can be adjusted 40 and 160. The CCD microscopic camera is USB interface sensor with 320×240 resolution. The focal distance was adjusted to get relatively clear images through the moving of the camera lens droved by lead screw in camera support. The camera len can also move around the rise screw rotation and small range of bobs for shooting the tool flank. The digital signals of each frame image from the CCD microscope camera were delivered to Sinumerik 840D CNC system by USB port.

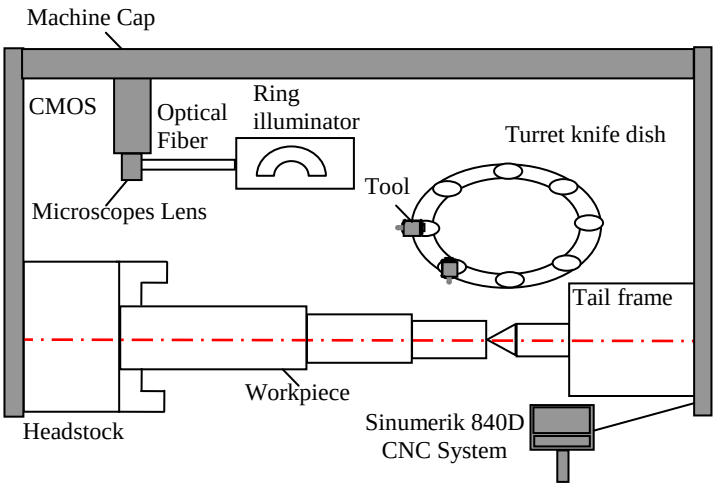


**Figure 4. Program Schematic of the Tool Wear Monitoring**

### 3.2. Image Acquisition and Feature Processing

The image acquisition part consists of light source, lens, digital camera and image acquisition card, the on-site installation testing is shown in Figure 5. The digital camera takes the picture of the target object and turn it into an image signal in the condition of lighting, then transmit to the image processing part by the image acquisition card. According to the requirements of the detected object, the seven geometric features of cutting tool and color feature (monitoring of the coating surface) need to be extracted, so the color CMOS camera FFMV-03MTC-CS is utilized for the experiment. The camera supports multiple images trigger mode, the trigger_mode_15 makes the camera collect the number of image (below 255) with the current frame rate via external trigger or software trigger, which is set by the parameter through trigger_mode register. The triggered camera can collect continuously, equivalent to trigger the camera and make it work in the free-running mode when the parameter is set to 0. Once triggered, N number of images will be collected with the exposure time set in the current shutter register and transmitted the image flows to the host at the current frame rate, then, the camera will be in the state of waiting for the next trigger. The any changes of the trigger_mode register will stop the current acquisition sequence. In fact, this model is still an asynchronous trigger mode, but not the free-running mode. And frame_rate register 0x83C will be turned off; the camera is placed in the extended shutter mode, so the maximum shutter time should be less than one in the current frame rate in practical applications. PLC was adopted to control the camera implement a series of operations, such as turn on, leaflets pictures, continuous shooting, pause, resume, single delivery, continuous transmission, stop, turn off *etc*[1].

 

**Figure 5. Measurement Set Mounted on the HTC2550hs**

The lens is selected in accordance with the shooting range and the resolution of the camera. The shooting range is calculated according to the Equation.15.

$$FOV = (D_P + L_V) \times (1 + \alpha) \tag{15}$$

where $FOV$ is shooting range, $D_P$ is the shooting object's size in this direction, $L_V$ is the object's movement in this direction, $\alpha$ is generally set to 10%, it is a amplification factor to ensure that the target image is not just at the edge. M5018-MP lens is used to get image with a resolution of 1024*768.The light source contains a annular angle light irradiation of the 45-degree angle OPT-RID70(outer diameter is 70mm, the inner diameter is 54mm) and a backlight source OPT-FL5050.

The tool's rake face image and flank face image can be acquired at the same time with the CCD industrial camera. The flow chart of tool wear monitoring and tool radius compensation is shown in Figure 6. In order to achieve and complete monitoring tool wear morphology in complex background conditions, the wear feature parameters were extracted, the dynamic real-time collection images were preprocessed. In the image preprocess, first of all, the clarity of the target's original image must be maintained and without destroying the useful information such as contour and edge, secondly, the noise interference was eliminated and the background unrelated to the object was removed. The acquired high-speed machining tool's image is shown in Figure 7.The median filter method and enhanced resolution, mean filter and image segmentation method in reference [20] was adopted to remove or reduce the noise and interference of the blade image because of complicated tool image background in high-speed machining. The tool's image adopted median filter method is shown in Figure 8 and the tool's image after histogram equalization is shown in Figure 9. The target area of interest was enhanced, the Signal to Noise Ratio (SNR) of the image quality was enhanced, and the enhanced tool's image is shown in Figure 10. The wear area boundary was accurately positioned, and the edge detection tool's image is shown in Figure 11. Three feature parameters of rake face were obtained by the calculation method in reference [23]. After precise positioning the flank wear boundary, the image was divided into B zone, N zone and C zone, the seven eigenvalues were measured using the microscope [24]. The feature extraction and feature measurement tool's image is shown in Figure 12.

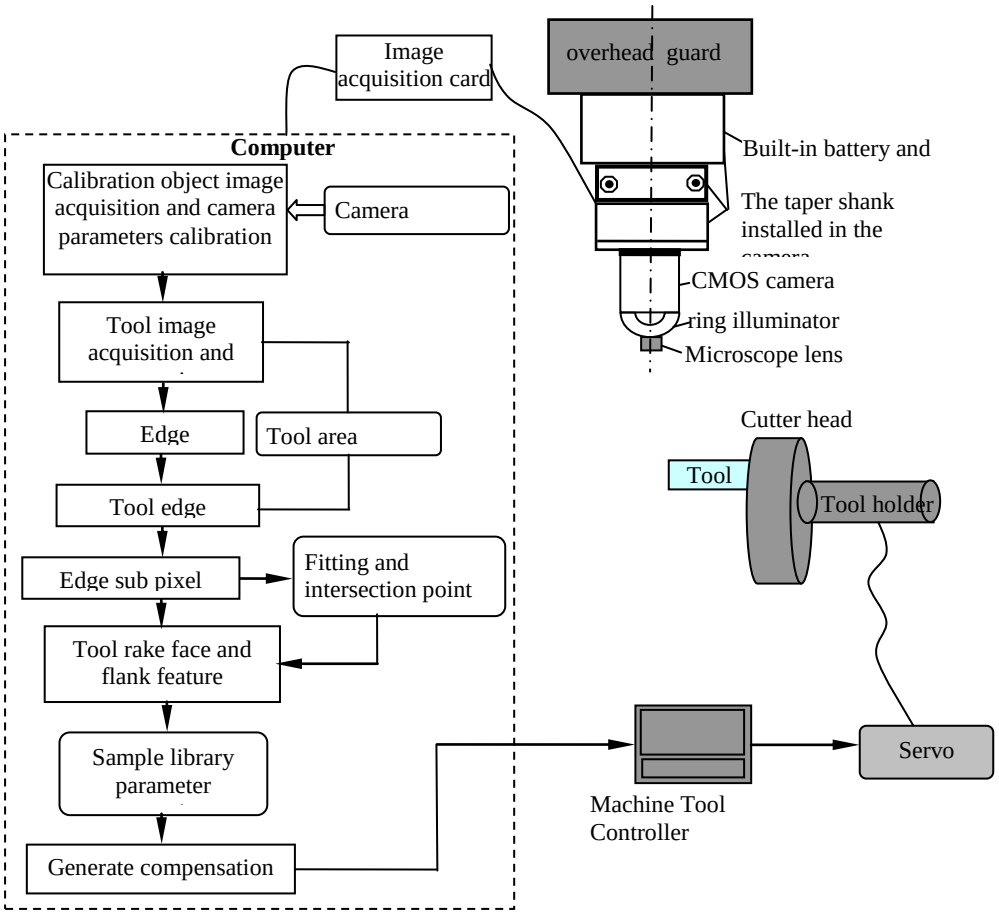


**Figure 6. Flow Chart of Tool Wear Monitoring and Tool Compensation**

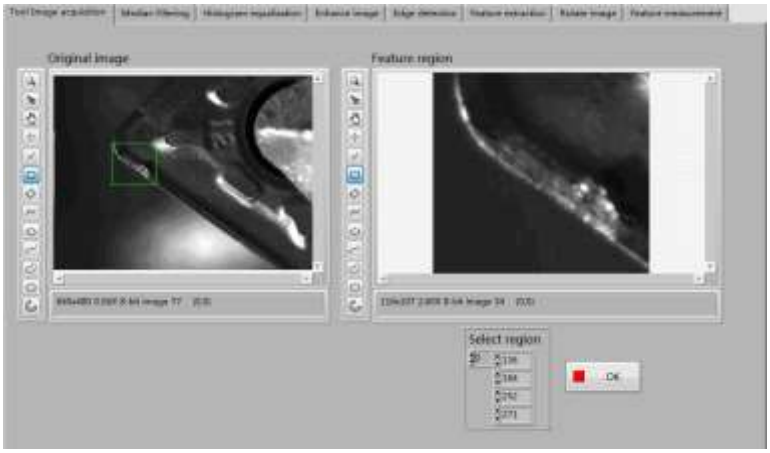


**Figure 7. The Acquired High-speed Machining Tool's Image**


**Figure 8. The Median Filtering Tool's Image**

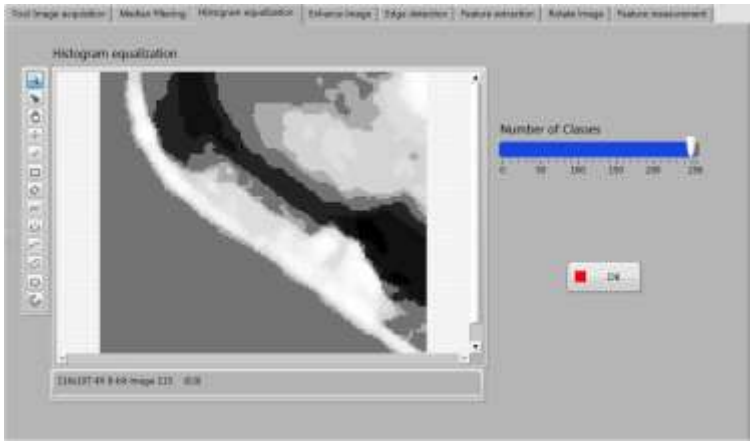


**Figure 9. The Tool's Image after Histogram Equalization**

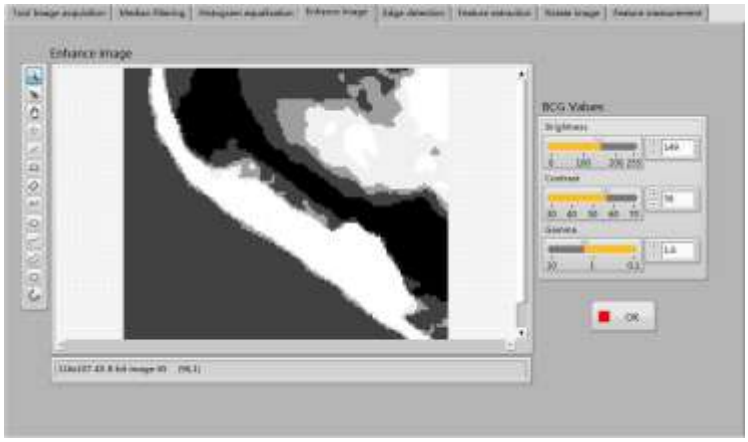


**Figure 10. The Enhanced Tool's Image**


**Figure 11. The Edge Detection Tool's Image**

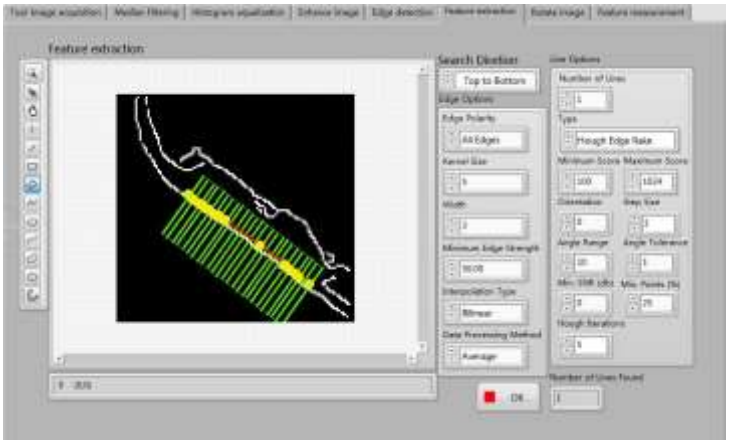


**Figure 12a. The Feature Extraction Tool's Image**

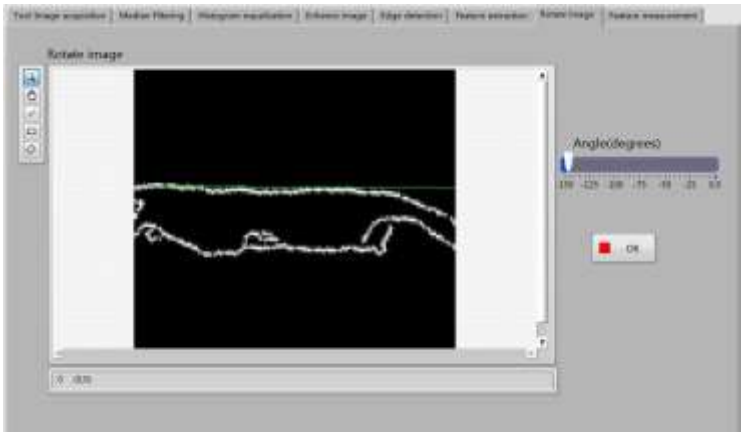


**Figure 12b. The Rotating Tool's Image**

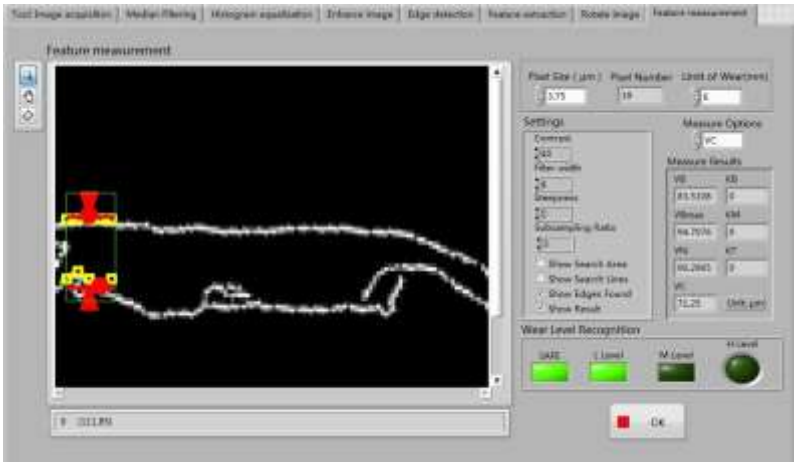


**Figure 12c. The Feature Measurement in C Zone Tool's Image**

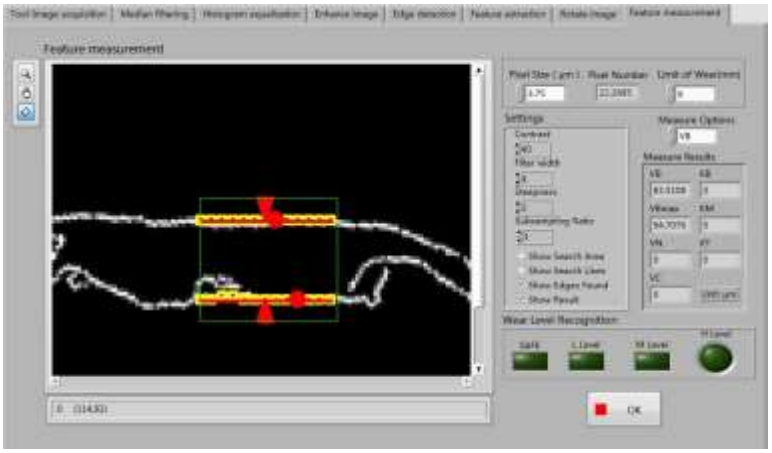


**Figure 12d. The Feature Measurement in B Zone Tool's Image**

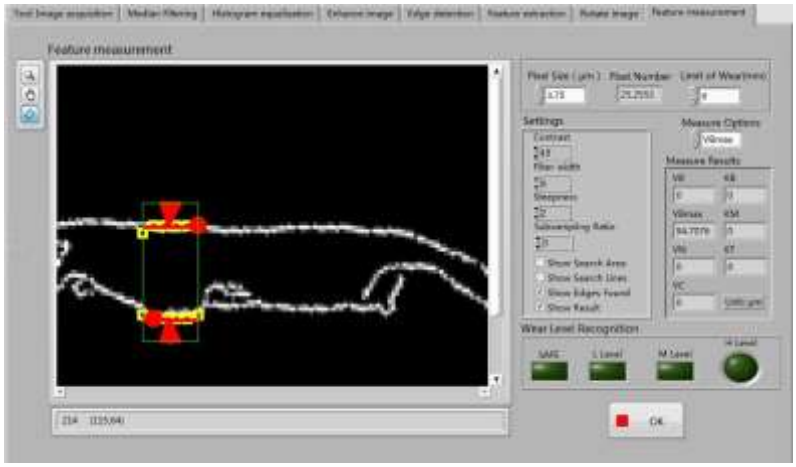


**Figure 12e. The Feature VBmax Measurement in B Zone Tool's Image**

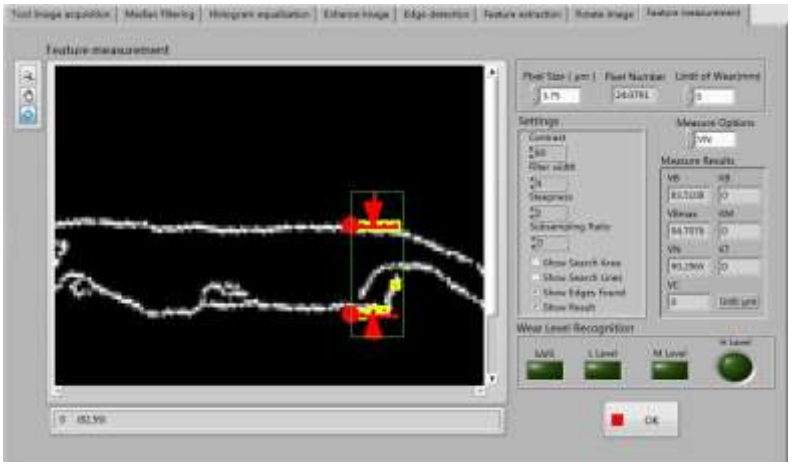

**Figure 12f. The Feature Measurement in N Zone Tool's Image**

### 3.3. Testing Calculation and Analysis

Seven testing sets are obtained by the above method, and each test set contains 10 group testing data and each group test data contains 7 feature parameters. Then the membership function values of each group were calculated separately. The wear levels were identified by the proposed multi-wear pattern recognition method as shown in Table 1. Its identification accuracy can get 98.6% comparing with the wear level using LDA method in Reference [17]. The identification results of wear level were shown in Figure13, the analysis results shown that the method can effectively identify the tool wear level and adapt to monitoring the tool wear level in a variety of conditions. The tool wear capacity was estimated to provide an important basis for tool radius compensation and bias parameter modification when the wear level is located in the L level; and the tool was replaced in time to prevent the tool enters into the H level when the wear level is located at the end of the M level.

**Table 1. Testing Results**

| Testing set | 1 | 2 | 3 | 4 | 5 | 6 | 7 |
|---|---|---|---|---|---|---|---|
| KB (μm) | 11 | 39 | 43 | 14 | 74 | 62 | 60 |
| KM (μm) | 8 | 21 | 24 | 9 | 45 | 34 | 32 |
| KT (μm) | 5 | 14 | 15 | 6 | 33 | 28 | 25 |
| VB (mm) | 0.08 | 0.23 | 0.27 | 0.14 | 0.41 | 0.37 | 0.35 |
| $VB_{max}$ (mm) | 0.12 | 0.28 | 0.32 | 0.21 | 0.47 | 0.39 | 0.38 |
| VN (mm) | 0.15 | 0.31 | 0.33 | 0.24 | 0.47 | 0.41 | 0.39 |
| VC (mm) | 0.13 | 0.26 | 0.29 | 0.16 | 0.25 | 0.35 | 0.26 |
| Membership function value | 0.14263 | 0.35248 | 0.36457 | 0.14869 | 0.75245 | 0.65243 | 0.64325 |
| Wear level | L | M | M | L | H | H | H |
| Wear level based on LDA | L | M | M | L | H | H | M |

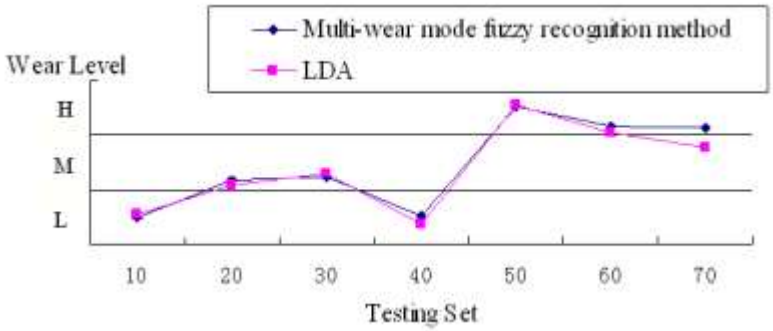


**Figure 13. Comparison Curve of Tool Wear Level Recognition**

## 4. Conclusions

In order to improve accuracy and efficiency of high-speed cutting tool wear monitoring and classification, the method was investigated to identify the tool wear level and estimate wear capacity based on machine vision and fuzzy statistical learning from theoretically and experimentally aspects in turning process. The following is a summary of findings from the present work:

(1) The monitoring method was proposed to identify the tool wear level and estimate wear capacity based on machine vision and fuzzy statistical learning. Wear feature parameters were extracted by analyzing the high-speed cutting tool wear morphology and wear mechanism. The feature vector of each worn tool was established, and the membership functions were designed, which correspond with low, medium and high wear level. The method represents the probability of belonging to the low, medium and high wear level.

(2) To achieve a more accurate result, the dynamic real-time collection images were preprocessed, and the median filter method and image segmentation method was adopted to remove or reduce the noise and interference of the blade image because of complicated tool image background in high-speed machining. The tool wear of rake face and flank face can be computed based on the detected wear edge points.

(3) The experimental work has demonstrated that the proposed monitoring method can be used successfully the tool wear in turning the shaft process. Experimental results shown that the proposed method can effectively identify the tool wear level, and the probability of L, M, H wear level was calculated, and the identification accuracy can get 98.6% exceed the LDA method identifying the wear levels in Reference [17].

(4) The tool wear capacity was estimated to provide an important basis for tool radius compensation and bias parameter modification when the wear level is located in the L level; and the tool was replaced in time to prevent the tool enters into the H level when the wear level is located at the end of the M level. The method of tool multi-wear mode feature representation and information processing provide new ideas for the multi-parameter monitoring of similar complex system, which have better theoretical foundation and application value.

## Acknowledgments

This work is supported by National Natural Science Foundation of China (Grant No. 51305124), Natural Science Foundation of Hebei Province (No. E2014202068) and Natural Science Foundation of Tianjin (No. 16JCYBJC19100).

# References

[1] Z. Yang, "Dynamic and Static Characteristics Monitoring Technology for High-speed CNC Machining Equipment based On Complex System Theory", Doctoral dissertation.Hebei University of Technology, **(2010)**.
[2] T. Segreto, A. Simeone and R. Teti, "Multiple sensor monitoring in nickel alloy turning for tool wear assessment via sensor fusion", Procedia CIRP, vol. 12, **(2013)**, pp. 85-90.
[3] Zhanqiang LIU and Xing AI, "Wear characteristics of cutting tools in high speed machining,Tribology", vol. 22, no. 6, **(2002)**, pp. 468-471.
[4] C.H. Lauro, L.C. Brandão, D. Baldo, R.A. Reis and J.P. Davim, "Monitoring and processing signal applied in machining processes-A review", Measurement, vol. 58, **(2014)**, pp. 73-86.
[5] M.S.H. Bhuiyan, I.A. Choudhury and M. Dahari, "Monitoring the tool wear, surface roughness and chip formation occurrences using multiple sensors in turning", Journal of Manufacturing Systems, vol. 33, no. 4, **(2014)**, pp. 476-487.
[6] Miho Klaic, Tomislav Staroveski and Toma Udiljak, "Tool wear classification using decision treesin stone drilling applications, A preliminary study", Procedia Engineering, vol. 69, **(2014)**, pp. 1326-1335.
[7] Bovic Kilundu, Pierre Dehombreux and Xavier Chiementin, "Tool wear monitoring by machine learning techniques and singular spectrum analysis", Mechanical Systems and Signal Processing, vol. 25, no. 1, **(2011)**, pp. 400-415.
[8] Muhammad Rizal, Jaharah A. Ghani, Mohd Zaki Nuawi and Che Hassan Che Haron, "Online tool wear prediction system in the turning process using an adaptive neuro-fuzzy inference system", Applied Soft Computing, vol. 13, no. 4, **(2013)**, pp. 1960-1968.
[9] Michał Szydłowski, Bartosz Powałka, Marcin Matuszak and Paweł Kochmański, "Machine vision micro-milling tool wear inspection by image reconstruction and light reflectance", Precision Engineering, vol. 44, **(2016)**, pp. 236-244.
[10] D.M. D'Addona, R. Teti, "Image data processing via neural networks for tool wear prediction", Procedia CIRP, vol. 12, **(2013)**, pp. 252-257.
[11] Bin Li, "A review of tool wear estimation using theoretical analysis and numerical simulation technologies", International Journal of Refractory Metals and Hard Materials, vol. 35, **(2012)**, pp. 143-151.
[12] Yi Wan, Zhanqiang LIU and Xing AI, "Tool wear patterns and mechanisms of solid cemented carbide in high-speed milling of aluminum alloy", Transactions of Nanjing University of Aeronautics & Astronautics, vol. 24, no. 2, **(2007)**, pp. 125-128.
[13] Shutao HUANG, Chunde JIA, Zenghui JIANG and Junyi YU, "Cutting performance and wear mechanism of tin coat cutter in high speed turn-milling", Journal of Harbin Institute of Technology, vol. 40, no. 9, **(2008)**, pp. 1501-1505.
[14] R.P. Martinho, F.J.G. Silva and A.P.M. Baptista, "Cutting forces and wear analysis of si3n4 diamond coated tools in high speed machining", Vacuum, vol. 82, no. 12, **(2008)**, pp. 1415- 1420.
[15] Yousheng LI, Jianxin DENG, Hui ZHANG and Jianfeng LI, "Wear mechanism of cemented carbide tool in high speed machining titanium alloy (Ti-6Al-4V)", Tribology, vol. 28, no. 5, **(2008)**, pp. 443-447.
[16] A. Datta, S. Dutta, S.K. Pal and R. Sen, "Progressive cutting tool wear detection from machined surface images using voronoi tessellation method", Journal of Materials Processing Technology, vol. 213, no. 12, **(2013)**, pp. 2339-2349.
[17] J. Barreiro, M. Castejón and E. Alegre, "Use of descriptors based on moments from digital images for tool wear monitoring. International", Journal of Machine Tools and Manufacture, vol. 48, no. 9, **(2008)**, pp. 1005-1013.
[18] P.C. Wanigarathne, A.D. Kardekar and O.W. Dillon, "Progressive tool-wear in machining with coated grooved tools and its correlation with cutting temperature", Wear, vol. 259, no. 7, **(2005)**, pp. 1215-1224.
[19] Yue ZHANG, "Research on tool wear inspection technology based on computer vision", Mechanical Engineering & Automation, Vol. 12, no. 4, **(2008)**, pp. 107-109.
[20] E. Aligiri, S.H. Yeo and P.C. Tan, "A new tool wear compensation method based on real-time estimation of material removal volume in micro-EDM", Journal of Materials Processing Technology, vol. 210, no. 15, **(2010)**, pp. 2292-2303.
[21] Chen Zhang and Jilin Zhang, "On-line tool wear measurement for ball-end milling cutter based on machine vision", Computers in Industry, vol. 64, no. 6, **(2013)**, pp. 708-719.
[22] M. Lanzetta, "A New Flexible High-resolution Vision Sensor for Tool Condition Monitoring", Journal of Materials Processing Technology, vol. 119, no. 1, **(2001)**, pp. 73-82.
[23] Y. Huang and Ty G. Dawson, "Tool Crater Wear Depth Modeling in CBN Hard Turning", Wear, vol. 258, no. 9, **(2005)**, pp. 1455-1461.
[24] J.A. Ghani, M. Rizal, M.Z. Nuawi, M.J. Ghazali and C.H.C. Haron, "Monitoring online cutting tool wear using low-cost technique and user-friendly GUI" , Wear, vol. 271, no. 9, **(2011)**, pp.2619-2624.

 

## Authors

**Zeqing Yang**, she received her B.S. degree in Mechanical Manufacture and Automation from Lanzhou Jiaotong University, China, in 2004, her M.S. degree in Vehicle Engineering from Lanzhou Jiaotong University, China, in 2007, and Ph.D. degree in Mechanical Manufacture and Automation from Hebei University of Technology, Tianjin, China, in 2010. Currently, she is an assistant professor at the School of Mechanical Engineering, Hebei University of Technology. Her research interests include visual monitoring technology, image processing and high precision CNC machine tool characteristics and control technology.

**Libing Liu**, she received her B.S. degree and M.S. degree in Mechanical Manufacture and Automation from Hebei University of Technology, China, in 1983 and 1995 respectively, and Ph.D. degree in Mechanical Manufacture and Automation from Tianjin University, China, in 1998. Since 2000, she has been a Full Professor at the School of Mechanical Engineering, Hebei University of Technology. Her research interests include digital integrated manufacturing technology and equipment, multi-source information intellisense technology and application.

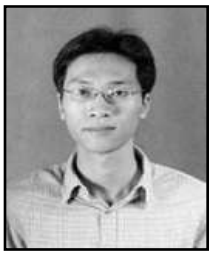

**Kai Peng**, he received her B.S. degree in Electromechanical Engineering from North-China Electric Power University in 2000, and M.S. degree and Ph.D degree in Measurement Technology and Instrument from Tianjin University,china, in 2004 and 2007 respectively. Since 2007, he has been a teacher at school of mechanical engineering, Hebei University of Technology. His research interests include machine vision and precision measuring.

**Shanshan Li**, she received her B.S. degree in Measurement Technology and Instrument from Hebei University of Technology, Tianjin, China, in 2014. She is currently a Master candidate in Measurement Technology and Instrument at the School of Mechanical Engineering, Hebei University of Technology. Her research interests include computer vision and image processing.

**Junfeng Zhang**, He received his B.E. degree in Measurement Technology and Instrument from Hebei University of Technology, Tianjin, China in 2014. He is currently a Master candidate in Instrument Science and Technology at the School of Mechanical Engineering, Hebei University of Technology. His research interests include machine tool vision monitoring and hardware circuit.

**Liya Gai**, she received her B.S. degree in Mechanical Manufacture and Automation from Shenyang University of Technology, China, in 1996, her M.S. degree in Mechanical Engineering from Jilin University, China, in 1999. Currently, she is a senior engineer at Shenyang No.1 Machine Tool Works of Shenyang

Machine Tool Group CO., LTD. Her research interests include high precision CNC machine tool.

 